

Mitigating LLM Hallucination via Behaviorally Calibrated Reinforcement Learning

Jiayun Wu^{1,2,†}, Jiashuo Liu^{1,†}, Zhiyuan Zeng^{1,3}, Tianyang Zhan¹, Wenhao Huang¹

¹ByteDance Seed, ²Carnegie Mellon University, ³Fudan University

Abstract

The deployment of Large Language Models (LLMs) in critical domains is currently impeded by the persistent phenomenon of hallucination—the generation of plausible but factually incorrect assertions. While scaling laws have driven significant improvements in general capabilities, recent theoretical frameworks suggest that hallucination is not merely a stochastic error but a predictable statistical consequence of training objectives that prioritize mimicking the data distribution over epistemic honesty. Standard RLVR paradigms, which predominantly utilize binary reward signals, inadvertently incentivize models to function as “good test-takers” rather than “honest communicators”, encouraging guessing whenever the probability of correctness exceeds zero. In this paper, we present an exhaustive investigation into *behavioral calibration*, which incentivizes the model to stochastically admit uncertainty by abstaining when it is not confident, thereby aligning the model’s behavior with its accuracy. We synthesize methodologies from recent advances to propose and evaluate training interventions that optimize strictly proper scoring rules for the model to output a calibrated probability of correctness. Our methods enable the model to either abstain from producing a complete response or to flag individual claims for which uncertainty remains. Utilizing the Qwen3-4B-Instruct model, our empirical analysis reveals that behaviorally-calibrated reinforcement learning allows smaller models to surpass frontier models in uncertainty quantification, which we demonstrate as a transferable meta-skill that can be decoupled from raw predictive accuracy. Trained on mathematical reasoning tasks, our model’s log-scale gain in Accuracy-to-Hallucination Ratio (0.806) exceeds that of GPT-5 (0.207) with a challenging in-domain evaluation (on BeyondAIME [7]). Moreover, in cross-domain factual QA (on SimpleQA [31]), our 4B LLM achieves a zero-shot calibration error on par with frontier models including Grok-4 and Gemini-2.5-Pro, even though its factual accuracy is much lower.

Date: December 24, 2025

Correspondence: Jiayun Wu@jiayunw@cmu.edu, Jiashuo Liu@liujiashuo.77@bytedance.com

1 Introduction

The rapid advancement of Large Language Models (LLMs) has been characterized by a relentless pursuit of accuracy on static benchmarks. However, as these systems are integrated into complex agentic pipelines [4, 12, 13, 35] and user-facing applications [3], the safety bottleneck has shifted from “can the model answer correctly” to “does the model know when it is uncertain or even wrong”. The phenomenon of hallucination—where models confabulate facts with high confidence—remains a stubborn artifact of the current post-training paradigm [16]. Despite the emergence of long CoT reasoning models, hallucinations persist, particularly in

domains requiring precise parametric knowledge [31] or multi-step logical deduction.

The prevailing hypothesis [16] attributes hallucination to a fundamental misalignment in the reward models used during Reinforcement Learning (RL). In standard Reinforcement Learning with Verifiable Rewards (RLVR), the reward function is typically binary: a response is graded as correct (+1) or incorrect (-1). Under this regime, a utility-maximizing agent is incentivized to generate a definitive answer as long as its internal probability estimate of correctness, p , is greater than zero. This creates a penalty for abstention, forcing the model to suppress uncertainty and masquerade guesses as facts. Consequently, models are trained to be “good test-takers”, who guess to maximize expected score, rather than “honest communicators” who abstain when confidence is low.

This work explores the theoretical and practical implementation of Behavioral Calibration, a framework recently formalized by Kalai et al. [16]. Behavioral calibration posits that a trustworthy model should dynamically adjust its refusal behavior based on a user-specified risk threshold t . Ideally, the model should output a substantive answer if and only if its confidence $p \geq t$, and otherwise output a refusal token (e.g., “I don’t know” or <IDK>). We implement this idea via reinforcement learning with custom reward functions to elicit behavior calibration. Specifically, we design and systematically compare three strategies:

1. **Explicit Risk Thresholding.** At training time, we randomly vary the risk tolerance t , inform the model of t in the prompt, and reward the model as follows: a correct answer yields a positive reward (+1), an answer of <IDK> incurs a neutral reward (0), and an incorrect answer yields a negative reward ($-t/(1-t)$) adaptive to the allowed risk. This scheme makes honest abstention valuable and incentivizes the model to calibrate its internal confidence. An ideal Bayesian model under this reward would answer if and only if its probability of correctness exceeds the risk tolerance threshold t .
2. **Verbalized Confidence.** Instead of conditioning the model on an external threshold, we train the model to explicitly output a scalar confidence score p alongside its response. For every risk threshold t , we compute the risk-adjusted reward in **Explicit Risk Thresholding** by abstaining when $p \geq t$. Assuming a prior distribution of the risk threshold t , we average the risk-adjusted reward over all possible thresholds. The derived average reward is a strictly proper scoring rule that incentivizes the model to report a confidence p that matches its true probability of correctness.
3. **Critic Value.** We investigate the efficacy of using the PPO Critic’s value function as an implicit confidence estimator. Since the Critic network minimizes the Brier score between the predicted value and the return of policy, it naturally converges to the probability of success. This strategy is a byproduct of Actor-Critic reinforcement learning without requiring the overhead of tokenized confidence generation.

According to user-defined risk preferences, we train policy models to either decline to provide a full response or to explicitly identify individual claims within a response that are assessed as uncertain. Through experiments on both domain-specific reasoning tasks and open-domain QA, we demonstrate that our approach substantially improves the model’s calibration and reduces hallucination without sacrificing accuracy. We evaluate hallucination mitigation using the Signal-to-Noise Ratio (SNR), defined as the ratio of accurate responses to hallucinated responses among instances in which the model provides an answer. Our empirical results are particularly striking given the small scale of our model. On the challenging in-domain BeyondAIME mathematical reasoning benchmark, our 4B-parameter model achieves a log-scale SNR gain of **0.806** when it adaptively refuses an entire response, substantially outperforming GPT-5 (**0.207**). When restricted to highlighting uncertainty at the level of individual claims, the same model attains a log-scale SNR gain of **0.183**, superior to **0.019** for Gemini-2.5-Pro. This indicates that smaller models can be trained to be strictly more self-aware of their limitations than their larger counterparts. In the zero-shot cross-domain setting SimpleQA, our model maintains calibration error rates comparable to frontier models like Grok-4 and Gemini-2.5-Pro, despite the natural deficit in absolute factual accuracy inherent to smaller parameter counts. Additionally, our analysis of the training dynamics reveals that the **Critic Value** emerges as a strong baseline for uncertainty estimation. Finally, the confidence estimates of our methods effectively function as a reward proxy for test-time scaling that improves over majority voting.

2 Related Work

Theoretical Investigations of Hallucination. The persistent prevalence of hallucinations in LLMs has prompted rigorous theoretical investigation into its causes. Recent literature suggests that hallucinations are not merely stochastic errors but are often a predictable artifact of the standard pre-training and post-training objectives [15, 16]. Specifically, accuracy-based benchmarks and standard Reinforcement Learning with binary correctness rewards implicitly incentivize guessing behavior. As long as the probability of correctness is non-zero, a utility-maximizing model will attempt an answer rather than abstain, thereby magnifying hallucination rates. These findings imply that hallucinations arise as a statistical effect of the misaligned evaluation metrics that fail to penalize confident errors. Consequently, there is a growing consensus for new training objectives that assign partial credit for uncertainty and explicitly penalize overconfident incorrect responses.

Hallucination Detection. Prior to mitigation, a significant body of work has focused on detecting hallucinations using post-hoc analysis of model behaviors. One branch of research exploits the statistics of the model’s output to identify uncertainty. For instance, measuring semantic entropy across sampled generations has proven effective in distinguishing confabulations from factual claims [10], while other works have explored the emergence of semantic calibration where models become calibrated on concepts despite being trained by next token prediction [21]. Parallel to output analysis, researchers have investigated internal model signals, such as activation patterns and embeddings, to detect hallucinations. Zhou et al. [37] leverages these internal states for detection and subsequent mitigation, while lightweight calibration methods have been proposed to assess trustworthiness over LLM generated responses using internal probes [14, 20].

Abstention and Self-Verification. Beyond passive detection, recent approaches aim to actively train models to recognize their own limitations and abstain from answering. Kapoor et al. [17] introduces a calibration fine-tuning strategy to explicitly assess their own responses when prompted by an uncertainty query, and output refusal tokens when uncertainty is high. Similarly, self-verification pipelines train models to critique their own outputs, using reinforcement learning to refine reasoning or trigger retries when errors are suspected [5, 19]. Advanced paradigms reinforce the generator and verifier jointly, creating a coupled system where the model learns to reason and verify simultaneously [36].

Verbalized Confidence. Our work is most closely related to the emerging field of verbalized confidence, where models are trained to express their uncertainty as scalar scores in natural language. Early work demonstrated that LLMs possess a latent ability to evaluate their confidence when prompted [25], though with a tendency for over-confident estimates. Lin et al. [18] calibrates such confidence estimates by supervised finetuning. More recently, reinforcement learning has been applied to optimize confidence expressions directly. Damani et al. [9], Stangel et al. [27] replace binary success rewards with proper scoring rules to calibrate the model’s confidence. These methods demonstrate that incentivizing honest uncertainty expression can improve calibration without sacrificing reasoning performance.

Test-Time Scaling with Confidence. As a downstream application, accurate confidence estimation enables test-time scaling strategies. Reliable confidence scores allow for more effective aggregation, where confidence-weighted voting outperforms simple majority voting [28]. Fu et al. [11] utilizes model-internal confidence to dynamically allocate compute resources during inference, prioritizing traces with higher confidence and filtering out low-quality reasoning paths.

Comparison with Related Work. We build on the foundational insights of using proper scoring rules in RL [9, 27], and introduce a behavioral abstention mechanism into the calibration process, which treats risk tolerance as a dynamic input. In contrast to prior work that often decouples confidence estimation from the decision of whether to answer, our approach trains the model to be sensitive to the user’s specific error tolerance. The model effectively learns the entire calibration curve simultaneously, inherently leading to adaptive abstention policy. Furthermore, our formulation unifies the reward design into the choice of the risk preference distribution, eliminating the need to manually tune sensitive hyperparameters balancing calibration

rewards against accuracy rewards [27]. Finally, we extend the framework of behavioral calibration [16] from the response level to the claim level, allowing models to precisely flag individual uncertain steps and offer fine-grained epistemic transparency that response-level strategies lack.

3 Methodology

In this section, we formalize methodologies for *behavioral calibration*. Our primary objective is to train a large language model that acts as both a competent test-taker and an honest communicator. We propose a framework where the model learns a single policy capable of adapting to a user-specified risk tolerance $t \in [0, 1]$. The framework allows for adaptive rejection of both the *entire response* (Section 3.2) and *individual claims* within the response (Section 3.3).

3.1 Objectives of Behavioral Calibration

For each prompt x and a risk threshold t , the model generates a response y , and decides on an action $a(t) \in \{\text{ANS}, \text{ABS}\}$ to ANSWER with response y or ABSTAIN using a special token $\langle \text{IDK} \rangle$. We specify four objectives of behavioral calibration.

1. **Adaptive Risk:** We aim to train a *single* policy model that satisfies calibration constraints across the entire spectrum of risk tolerance $t \in [0, 1]$. The model must be user-adjustable; given a threshold t , the model should automatically adjust its abstention strategy without retraining.
2. **Accuracy Preservation:** The calibration mechanisms must not degrade the model’s inherent ability. Specifically, at $t = 0$ (maximum risk tolerance), the accuracy of the calibrated model should match or exceed that of the baseline model finetuned by standard RL.
3. **Hallucination Reduction:** As the risk threshold t increases, the hallucination rate should monotonically decrease, ideally approaching zero as $t \rightarrow 1$. We quantify hallucination mitigation by **Signal-to-Noise Ratio** ($\text{SNR}(t)$), defined as the ratio of accuracy to hallucination rate under a specified risk preference t . Let $\text{valid}(y)$ be an indicator for the correctness of the response. The Accuracy $\text{Acc}(t)$, Hallucination $\text{Hal}(t)$, and $\text{SNR}(t)$ for a given risk threshold t are formally defined as:

$$\text{Acc}(t) = \mathbb{E}[\text{valid}(y) \wedge a(t) = \text{ANS}], \quad \text{Hal}(t) = \mathbb{E}[\neg \text{valid}(y) \wedge a(t) = \text{ANS}], \quad \text{SNR}(t) = \frac{\text{Acc}(t)}{\text{Hal}(t)}.$$

As t increases, a significant increase in $\text{SNR}(t)$ indicates effective hallucination mitigation and the model’s capability to distinguish between correct and incorrect responses. We extend the definition of SNR to an interval of risk thresholds $t \in I$ by averaging the accuracy and hallucination across the risk spectrum.

$$\text{SNR}(I) = \frac{\int_{t \in I} \text{Acc}(t) dt}{\int_{t \in I} \text{Hal}(t) dt}.$$

Our final evaluation focuses on the gain of the SNR over the entire spectrum $t \in [0, 1]$ relative to the risk-free baseline at $t = 0$.

$$\text{SNR-Gain} = \log \left(\frac{\text{SNR}([0, 1])}{\text{SNR}(0)} \right). \quad (1)$$

4. **Quantitative Calibration:** The model’s accuracy and abstention rates should satisfy two quantitative metrics for calibration.

The **True Positive** constraint requires that among the questions the model chooses to answer, the proportion of correct answers must be at least the stated confidence threshold t :

$$\text{TP}(t) = \mathbb{E}[\text{valid}(y) \mid a(t) = \text{ANS}] \geq t.$$

The **False Negative** constraint ensures the model is not overly conservative. Among the questions the model chooses to abstain from, the proportion of questions it *could* have answered correctly (at $t = 0$) must be lower than t :

$$\text{FN}(t) = \mathbb{E}[\text{valid}(y) \mid a(t) = \text{ABS}] \leq t$$

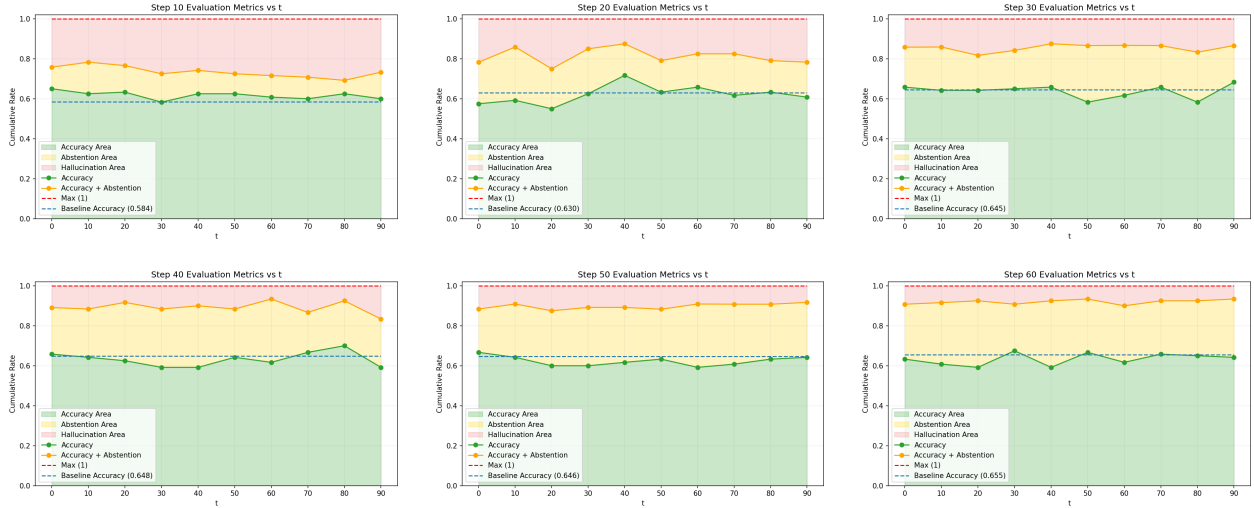


Figure 1 Accuracy, hallucination, and abstention rates across the training progress (Step 10, 20, 30, 40, 50, and 60) of **Explicit Risk Thresholding**. Base model: Qwen3-4B-Instruct. Trained by GRPO on the DAPO-Math-17k dataset [33]. Evaluated on AIME 2024. Baseline is trained with the standard binary reward.

3.2 Three Strategies for Behavioral Calibration

We design and systematically compare three strategies for behaviorally calibrated RL.

3.2.1 Explicit Risk Thresholding

A straightforward approach to induce calibrated behavior is to explicitly condition the model on the risk threshold t . We explicitly instruct the model on the scoring rules with the prompt from Kalai et al. [16]:

“Answer only if you are $> t$ confident, since mistakes are penalized $t/(1-t)$ points, while correct answers receive 1 point, and an answer of $\langle \text{IDK} \rangle$ receives 0 points.”

During the post-training phase, for every training instance, we sample a risk threshold t from a uniform distribution $t \sim \mathcal{U}(0, 1)$. The reward function R is formulated as:

$$R(a, y, t) = \begin{cases} +1 & \text{if } a = \text{ANS} \wedge \text{valid}(y) \\ 0 & \text{if } a = \text{ABS} \\ -\frac{t}{1-t} & \text{if } a = \text{ANS} \wedge \neg \text{valid}(y) \end{cases} \quad (2)$$

However, our preliminary experiments indicate several limitations of the approach (Figure 1). The objectives of behavioral calibration in Section 3.1 are not satisfied. The model fails to achieve **Adaptive Risk**. The refusal rate and hallucination rate proved insensitive to the specific prompt input t during inference. Second, it violates **Accuracy Preservation**. The policy tends to over-reject even at $t = 0$, often leading to performance below the baseline. Third, **Hallucination Reduction** is not achieved. Although the absolute hallucination rate reduces as training progresses, the Signal-to-Noise Ratio (SNR) does not positively correlate with the risk threshold t , resulting in a near-zero SNR-Gain. Note that, in Figure 1, SNR is visually represented by the ratio of the green area (Accuracy) to the red area (Hallucination). **Quantitative Calibration** also fails for $t = 1$ ($\text{TP}(1) < 1$) where the model is over-confident. In summary, explicitly sampling t creates a noisy optimization landscape where the model struggles to learn a coherent strategy for adaptive conditions from $t = 0$ to $t = 1$.

3.2.2 Verbalized Confidence

To overcome the instability of explicitly sampling risk thresholds, we prompt the model to explicitly output a scalar confidence score p along with its answer. Rather than conditioning on an input t , we make a post-hoc

decision to answer or abstain: abstain if and only if $p < t$.

$$a(t, p) = \text{ABS if } p < t \text{ else ANS.}$$

The key innovation is deriving the reward function by integrating the behavioral calibration reward over some prior distribution of risk thresholds. This transforms the training objective from conditional optimization (with sampled thresholds) into optimization for a proper scoring rule of verbalized confidence.

Formally, assume a distribution of risk tolerance supported on $(0, 1)$ which cumulative distribution function is denoted as $u(t)$. For each $t \in [0, 1]$, we scale the reward in Equation (2) to be bounded:

$$R(a, y, t) = \begin{cases} +1 & \text{if } a = \text{ANS} \wedge \text{valid}(y) \\ 2t - 1 & \text{if } a = \text{ABS} \\ -1 & \text{if } a = \text{ANS} \wedge \neg \text{valid}(y) \end{cases}$$

Then we average the risk-adjusted reward across all risk thresholds.

$$R_u(y, p) = \int_{t=0}^1 R(a(t, p), y, t) du(t) = 2 \cdot \text{valid}(y) \cdot \int_0^p du(t) + 2 \int_p^1 t du(t) - 1.$$

One can verify that R_u is a strictly proper scoring rule if the prior risk distribution $u(t)$ has positive density anywhere. A strictly proper scoring rule implies that the expected reward is maximized exactly when $p = \mathbb{E}[\text{valid}(y)]$.

Uniform Distribution. Assuming a uniform distribution of risk preference $t \sim \mathcal{U}(0, 1)$, the resulting average reward function is analogous to the Brier score.

$$R_{\text{Brier}} = 2p \cdot \text{valid}(y) - p^2. \quad (3)$$

This reward function can be decomposed into the sum of a correctness reward and the Brier score of the confidence: $R_{\text{Brier}} = \text{valid}(y) - (p - \text{valid}(y))^2$. Intuitively, the reward incentivizes the model to maximize prediction accuracy while simultaneously calibrating its stated confidence.

Beta Distribution. We consider a risk threshold distribution which emphasizes performance at the extreme ends of the risk spectrum—specifically the “test-taker” mode ($t \approx 0$) and the “fully honest” mode ($t \approx 1$). We utilize a truncated Beta(0, 0) distribution with density $du(t) \propto \frac{1}{t(1-t)}$ for $\epsilon < t < 1 - \epsilon$. Integrating the reward over this distribution yields a cross-entropy style reward function:

$$R_{\text{CE}} = \left(\log \frac{1 - \epsilon}{\epsilon} \right)^{-1} \left[\text{valid}(y) \cdot \log \frac{p'}{\epsilon} + (1 - \text{valid}(y)) \cdot \log \frac{1 - p'}{1 - \epsilon} \right], \quad (4)$$

where $p' = \text{clip}(p, \epsilon, 1 - \epsilon)$. This formulation imposes stronger penalties for overconfidence on wrong answers and underconfidence on correct answers.

3.2.3 Critic Value

As an alternative to generating confidence tokens, we explore a discriminative approach using the critic network of the PPO (Proximal Policy Optimization) algorithm. The critic network estimates the value function by minimizing the Brier score with the correctness reward, resembling **Verbalized Confidence** with a uniform prior of risk thresholds. Theoretically, the Critic is naturally trained to be a calibrated predictor of the expected accuracy. Therefore, we use the output of the PPO Critic at the final token directly as the confidence score. This method proves as a strong baseline.

3.3 Behavioral Calibration for Individual Claims

Further, we extend the framework of behavioral calibration to individual claims comprising the complete response. However, several subtle caveats impede a direct extension:

- Directly replacing an individual claim with a special token <IDK> often produces an incohesive response. For instance, steps in a mathematical solution are typically interdependent. Therefore, we propose to output the complete response while signifying abstention behavior by visually highlighting the uncertain claim in the user interface.
- Defining both correctness and confidence is ambiguous for intermediate steps within a response. For example, a reflective step in COT might correctly identify an error in a preceding incorrect claim. While this reflection might confidently identify the fault, it may indicate a lower confidence for a successful solution. To circumvent this inherent ambiguity, we disregard the intermediate COT steps and focus on the abstention behavior of the final solution.
- Explicit correctness annotations for the individual claims are absent. Therefore, we design a learning objective derived solely from the final outcome. Nevertheless, we demonstrate that our approach yields calibrated confidence estimates for these intermediate steps through weak supervision from the final outcome.

For the formal setup, we systematically prompt the model to reason privately before generating a final response that is structured into discrete steps. Specifically, for a given user prompt x , the model generates a final response $y = (y_1, y_2, \dots, y_N)$ composed of N individual claims, where N is determined dynamically by the model. For each claim y_i and a user-specified risk threshold t , the model must select an action $a_i(t) \in \{\text{ANS}, \text{ABS}\}$, determining whether to assert the claim (ANS) or to highlight it as uncertain (ABS). The ground-truth correctness of each claim y_i is denoted by $\text{valid}(y_i)$, which is determined by an LLM Judge in our experimental evaluation.

3.3.1 Verbalized Confidence

We instruct the model to explicitly output a confidence score p_i for each individual claim y_i . The model executes the abstention action (ABS) if and only if $p_i < t$. Furthermore, the model is prompted to provide a concise explanation justifying the reported confidence and identifying the source of uncertainty. We instruct the model to encapsulate each claim in HTML format, as illustrated in [Figure 2](#).

Since only the final outcome is annotated, we must aggregate the claim-level confidence scores into an overall response confidence. This aggregated confidence is subsequently used to post-train the model by our previous reward function derived from the proper scoring rule.

1. **Product Aggregation.** The most straightforward aggregation takes the product of the claim-level confidence scores ($p = \prod_i p_i$). This method is predicated on two assumptions: (i) the correctness events of individual claims are independent, and (ii) the final outcome is correct if and only if all claims are correct. Empirically, we find that the independence assumption is frequently violated, as confidence estimates across different steps of the same response tend to be highly correlated (e.g., incorrect responses often contain multiple errors). Consequently, while the response-level confidence may achieve calibration, the claim-level confidence is often over-confident. For instance, if a 10-step, incorrect response has a uniform claim-level confidence of 80% (over-confident), the product aggregation yields a response-level confidence of 11%, which is closer to a calibrated value.
2. **Minimum Aggregation.** We also investigate aggregation by taking the minimum of all claim-level confidence scores ($p = \min_i p_i$). For the previous example, this method requires that the confidence of the most uncertain claim be 11% to yield the same response-level confidence. Therefore, minimum aggregation incentivizes the model to allocate low confidence to the most fault-prone step.

Utilizing the aggregated confidence from either the product or minimum strategy, the model is subsequently post-trained using the Brier score reward function as defined in [Equation \(3\)](#).

```

User Prompt:
Let A, B, C, and D be point on the hyperbola  $x^2/20-y^2/24=1$  such that ABCD is a rhombus whose diagonals intersect at the origin. Find the greatest real number that is less than  $BD^2$  for all such rhombi.

Response:
[COT] (OMITTED)
Solution:
<Confidence
  value=1
  text="Completely derived using parametrization and constraints of hyperbola and orthogonality. All steps follow from standard parametric equations and trigonometric identities."
>
The hyperbola  $x^2/20-y^2/24=1$  is parametrized by  $x=20\sec\theta$ ,  $y=24\tan\theta$ . For a rhombus with diagonals intersecting at origin and perpendicular, the vertices are symmetric, so vectors A and B must satisfy  $A\cdot B=0$ . This leads to the equation  $24\sin\theta\sin\phi=-20$ , so  $\sin\theta\sin\phi=-65$ . For real solutions,  $|\sin\phi|\geq 65$ , and  $|\cos\phi|\leq 11/6$ , so  $\tan 2\phi\geq 1125$ . Then  $BD^2=4(x^2+y^2)=80+176\tan 2\phi\geq 80+176\cdot 1125=80+400=480$ . Equality is approached as  $|\sin\phi|\rightarrow 5/6$ , but for finite points, strict inequality holds. Therefore, for all such rhombi,  $BD^2>480$ , so the greatest real number strictly less than  $BD^2$  for all such rhombi is 480.
</Confidence>
<Confidence
  value=1
  text="The derivation is consistent and relies on correct hyperbola parametrization and trigonometric identities. The constraint from orthogonality is correctly transformed. The minimal value is correctly computed and the strict inequality in finite cases is justified."
>
The derivation of the condition from orthogonality and hyperbola parametrization is correct and fully checks out. The bound on  $\tan 2\phi$  is correct based on the sine constraint and the identity  $\tan 2\phi=\sec 2\phi-1$ . The minimal value computation  $80+176\cdot(25/11)$  is accurate and correct.
</Confidence>
<Confidence
  value=0.95
  text="Uncertainty: The problem's phrasing 'greatest real number that is less than  $BD^2$  for all such rhombi' might be interpreted differently - e.g., whether the rhombus must be bounded or if degenerate cases are allowed. However, in context and given that the limit case leads to unbounded points (infinite coordinates), the finite rhombi are considered, so the strict inequality  $BD^2 > 480$  holds for all non-degenerate finite cases. The conclusion about the greatest such number being 480 is sound in that setting."
>
There is a small risk in interpreting whether degenerate or infinite points are allowed - but the hyperbola's parametrization excludes infinite points in the domain, so all valid rhombi have finite coordinates and thus  $BD^2>480$ . The conclusion about the supremum being 480 is therefore valid.
</Confidence>
Answer:480

```

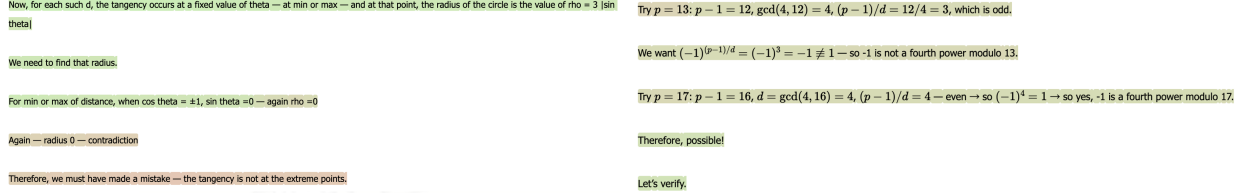
Figure 2 Sample output of Verbalized Confidence for individual claims from Qwen3-4B-Instruct-confidence-min.

3.3.2 Critic Value

Since the critic network of PPO intrinsically computes a token-level value, it is plausible to interpret this value function as the token-level confidence for the intermediate steps of the model’s output. However, because the critic network minimizes the Brier score relative to the *final outcome* reward, the resulting value function reflects the model’s confidence in the correctness of the final outcome conditional on the steps thus far, rather than confidence in the correctness of the current step itself. Our preliminary experiments confirm that this misaligned optimization objective impedes the extension of **Critic Value** as a confidence measure for individual claims.

We observe that **Critic Value** in intermediate steps essentially functions as a semantic classifier rather than an uncertainty verifier. For instance, in mathematical problems, the value function decreases when a contradiction is detected, when a suboptimal approach (e.g., enumeration, guessing) is employed, or when limited progress is achieved as the token budget is consumed. Crucially, the value function fails to decrease precisely where the underlying error occurs that subsequently leads to the contradiction. Conversely, the value function increases when a conclusion is verified or a promising approach is adopted. However, this increase does not register at the prior steps that led to the verified conclusion. Two samples are presented in Figure 3. This disparity arises because the value function is designed to estimate the probability of success for the final solution rather than the probability of correctness for the current step.

4 Experiments



(a) Confidence decreases at contradiction.

(b) Confidence increases at verification.

Figure 3 Sample output of **Critic Value** as token-level confidence. The continuous confidence is visualized with a color gradient scale, ranging from red (0% confident) to green (100% confident). Evaluated on AIME-2024.

4.1 Training Setup

We apply behavioral calibration to finetune **Qwen-3-4B-Instruct-2507** [30]. We use the PPO algorithm by default for reinforcement learning. We use GRPO [26] to train **Verbalized Confidence** with Beta distribution as the prior risk preference, because we discover improved training stability specifically for this reward design. We train our methods on the DAPO-Math-17k dataset from Yu et al. [33].

We compare **Verbalized Confidence** and **Critic Value** in response-level evaluations, while **Verbalized Confidence** is exclusively adopted in the claim-level evaluations. We present the following variants of our strategies:

- **Qwen3-4B-Instruct-PP0**: The baseline model finetuned with the standard binary correctness reward by the PPO algorithm.
- **Qwen3-4B-Instruct-Confidence-Brier**: **Verbalized Confidence** with uniform distribution as the prior of risk threshold. Trained for the response-level confidence.
- **Qwen3-4B-Instruct-Confidence-CE**: **Verbalized Confidence** with Beta distribution as the prior of risk threshold. Trained for the response-level confidence.
- **Qwen3-4B-Instruct-PP0-Value**: **Critic Value** built upon the PPO algorithm.
- **Qwen3-4B-Instruct-Confidence-Prod**: **Verbalized Confidence** with uniform distribution as the prior of risk threshold. Trained for the aggregated confidence by taking the product of individual claim-level confidence scores.
- **Qwen3-4B-Instruct-Confidence-Min**: **Verbalized Confidence** with uniform distribution as the prior of risk threshold. Trained for the aggregated confidence by taking the minimum of individual claim-level confidence scores.

Additionally, we include for reference several frontier models by directly prompting them to output **Verbalized Confidence** for both the complete response and individual claims. The evaluation includes a series of models from GPT [22–24], Claude-Sonnet [2], Grok [32], Gemini [8], GLM [1, 34], Qwen3 [30], and Kimi [29]. The comparison positions our 4B model relative to much larger models in terms of both accuracy and calibration.

4.2 Quantitative Evaluation of Confidence Calibration

We evaluate the the model’s confidence estimates, focusing on the behavioral calibration of their resulting abstention policy. First, we measure the standard calibration of the confidence estimates with respect to the ground-truth correctness outcome.

- **Smoothed ECE (smECE)**: Standard Expected Calibration Error (ECE) is computed by comparing the model’s reported confidences with actual accuracy in bins. However, standard ECE is biased and sensitive to bin count. We use smooth ECE [6], which utilizes kernel density estimation to smooth the observations and provide a theoretically-sound calibration measure.

Table 1 Response-level evaluation of confidence calibration on BeyondAIME [7].

Model	SNR Gain \uparrow	Conf AUC \uparrow	Abs Acc \uparrow	smECE \downarrow	Brier \downarrow	NLL \downarrow	Pred Acc \uparrow
Qwen3-next-80b-a3b-thinking	0.006	0.496	0.557	0.408	0.425	1.826	0.557
GLM-4.5	0.016	0.519	0.536	0.440	0.449	1.971	0.532
Qwen3-max	0.043	0.678	0.540	0.453	0.413	1.583	0.537
Gemini-2.5-Pro	0.071	0.699	0.553	0.431	0.387	1.443	0.544
Qwen3-4B-Instruct	0.084	0.715	0.338	0.632	0.599	2.316	0.291
Kimi-K2-0905	0.087	0.678	0.385	0.575	0.529	2.004	0.355
Qwen3-4B-instruct-ppo	0.101	0.786	0.388	0.560	0.518	1.873	0.361
GPT-oss-120b	0.154	0.703	0.497	0.419	0.402	1.415	0.436
GPT-5	0.207	0.706	0.718	0.160	0.208	0.719	0.680
o4-mini	0.515	0.738	0.698	0.164	0.241	0.845	0.527
Qwen3-4B-Instruct-confidence-min	0.683	0.863	0.703	0.220	0.194	0.606	0.384
Qwen3-4B-instruct-confidence-brier	0.802	0.902	0.782	0.177	0.161	0.527	0.395
Qwen3-4B-Instruct-confidence-prod	0.806	0.883	0.766	0.166	0.166	0.516	0.385
Qwen3-4B-Instruct-confidence-ce	1.097	0.854	0.771	0.174	0.179	0.722	0.364
Qwen3-4B-Instruct-ppo-value	1.202	0.881	0.797	0.061	0.141	0.436	0.387

- **Brier Score:** The mean squared error between the model’s confidence p and the outcome (1 for correct, 0 for incorrect).
- **Negative Log-Likelihood (NLL)** of correctness outcomes assuming the probability of correctness is given by the confidence p .

Second, we assess effective hallucination mitigation by the model’s discrimination between correct and incorrect responses, and accurate rejection of inaccurate responses.

- **Confidence AUC:** Area under the ROC curve by treating abstention as a classification task with estimated confidence. While ECE measures the alignment of average confidence with average accuracy, Confidence AUC is the critic metric for evaluating models’ ability to distinguish “knowns” from “unknowns”. It measures the probability that a correct answer is assigned a higher confidence score than an incorrect one. Crucially, AUC is independent of the risk threshold and the absolute problem-solving accuracy, making it fair for comparing weak and strong models.
- **SNR Gain:** Considering confidence estimates as the signal for rejection, we evaluate the policy’s Signal-to-Noise Ratio (SNR), defined as the ratio of accuracy to hallucination. As the risk threshold t increases, we expect reduction in hallucination which should cause increase in SNR. Therefore, our metric of interest is the gain of SNR across the spectrum of risk thresholds $t \in [0, 1]$ relative to the baseline at $t = 0$. Equation (1) provides the formal calculation of the SNR Gain.
- **Abstention Accuracy:** The proportion of responses that abstain from incorrect answers or answer with correct answers. Assume abstention with confidence below 0.5.

Finally, we measure the model’s raw accuracy in the risk-free setting ($t = 0$) for reference.

- **Predictive Accuracy:** The standard accuracy of problem solving assuming no abstention.

Math benchmarks have become saturated by frontier models. Therefore, we utilize BeyondAIME [7], which is composed of 100 ultra-hard mathematical problems with difficulty equal to or exceeding the hardest problems in AIME. Sourced from mathematical competitions, the problems are then systematically revised by specialists to be resistant to contamination. All answers are non-trivial positive integers, allowing for deterministic programmatic verification. This serves as the primary testbed for our model, which is post-trained on math data. It measures whether the model can calibrate its confidence on tasks it is explicitly trained to solve.

4.2.1 Response-Level Evaluation

We first evaluate the confidence estimates for the entire response. The results are in Table 1. Both **Verbalized Confidence** and **Critic Value** demonstrate significantly higher Confidence AUC and SNR Gain compared to the instruct model and other frontier models. The confidence scores reported by our methods possess the strongest capability to discriminate between correct and incorrect responses. The aggregated confidence from claim-level **Verbalized Confidence** exhibits performance metrics comparable to those directly producing a response-level confidence score. Figure 4 reveals a strong correlation between confidence and accuracy for our methods. A similar phenomenon is observed in GPT-5 and o4-mini. Conversely, in other frontier models and the untrained Qwen3 instruct model, accuracy shows negligible variation with respect to confidence. We demonstrate that post-training can effectively stimulate the model’s ability to accurately report confidence, which is a capability currently present exclusively in OpenAI series models.

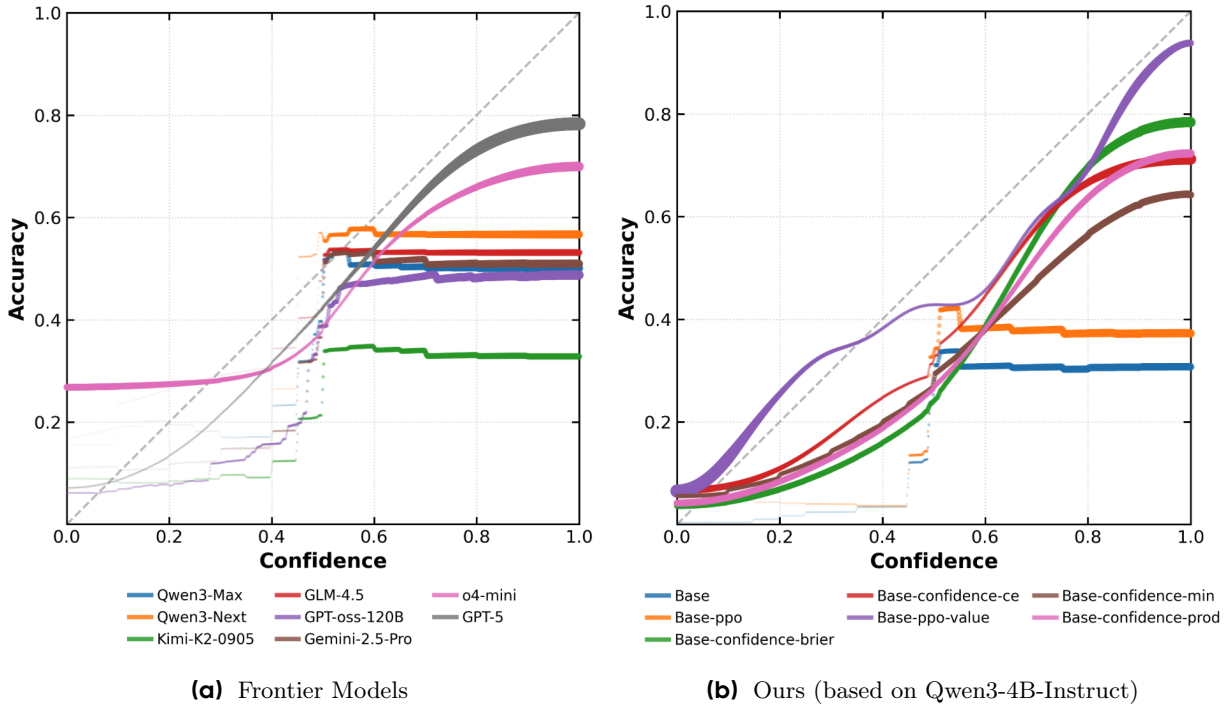


Figure 4 The calibration diagram for response-level stated confidence on BeyondAIME. The size of curves indicates density.

Method Comparison. In Table 2, We compare several variants of our methods on AIME-2024 and AIME-2025, whose difficulty aligns better with the capacity of Qwen3-4B-Instruct. **Verbalized Confidence** achieves the overall optimal calibration performance, as measured by Confidence AUC and smECE, when reward calculation uses a uniform distribution of risk thresholds (Confidence-Brier). On the other hand, a Beta distribution for the risk preference yields the optimal SNR Gain (Confidence-CE), implying the most aggressive mitigation of hallucination under stringent risk tolerance. **Critic Value** serves as a strong baseline with respect to the smECE metric.

4.2.2 Claim-Level Evaluation

The ground-truth correctness of individual claims is established by GPT-5 as Judge. The Judge is provided with the user prompt, the model solution, and the final answer’s ground-truth label. The Judge is then instructed to parse the claims from the HTML-formatted solution and assess the correctness of each extracted claim. We evaluate the behavioral calibration of the model’s claim-level abstention policy. The results are presented in Table 3.

Table 2 Response-level evaluation of confidence calibration on AIME.

Model	AIME-2024				AIME-2025			
	smECE↓	Conf AUC↑	SNR Gain ↑	Pred Acc↑	smECE↓	Conf AUC↑	SNR Gain ↑	Pred Acc ↑
Confidence-Brier	0.032	0.955	1.153	0.755	0.077	0.951	1.097	0.621
PPO-Value	0.070	0.909	1.051	0.702	0.042	0.938	1.105	0.627
Confidence-CE	0.075	0.894	1.320	0.701	0.084	0.900	1.352	0.638
PPO Only	0.223	0.877	0.205	0.705	0.301	0.886	0.213	0.608
Qwen3-4B-Instruct	0.330	0.787	0.177	0.590	0.450	0.836	0.153	0.466

Table 3 Claim-level evaluation of confidence calibration on BeyondAIME.

Model	SNR Gain ↑	Conf AUC ↑	Abs Acc ↑	smECE ↓	Brier ↓	NLL ↓	Pred Acc ↑
Qwen3-max	0.018	0.717	0.889	0.132	0.106	0.469	0.889
Gemini-2.5-Pro	0.019	0.719	0.891	0.130	0.104	0.449	0.891
Qwen3-4B-Instruct	0.027	0.617	0.563	0.456	0.419	1.809	0.558
GLM-4.5	0.029	0.676	0.719	0.294	0.260	1.027	0.719
o4-mini	0.068	0.601	0.774	0.210	0.211	0.887	0.770
Qwen3-4B-Instruct-confidence-prod	0.183	0.741	0.526	0.311	0.305	0.930	0.497
Qwen3-4B-Instruct-confidence-min	0.301	0.788	0.616	0.258	0.251	0.810	0.537

Through weak supervision from the final outcome, the post-trained Qwen3 models demonstrate a significant improvement in behavioral calibration for intermediate steps across all measured metrics compared to the base instruct model. Furthermore, Minimum aggregation of claim-level confidence proves superior to Product aggregation at the claim level, though the latter method achieves better calibration at the response level (Table 1). Compared to frontier models, **Verbalized Confidence** mitigates hallucination more effectively, evidenced by advantage in SNR Gain and Confidence AUC. Frontier models exhibit superiority in metrics of standard calibration, including smECE, Brier, and NLL. However, Figure 5 reveals that this is attributable to higher overall accuracy rather than superior confidence estimation. For frontier models, the accuracy is nearly independent of the stated confidence. In contrast, **Verbalized Confidence** yields informative confidence scores which monotonically increase with the empirical accuracy.

4.3 Criteria of Behavioral Calibration

We evaluate the behavioral calibration objectives in Section 3.1 on BeyondAIME. The results confirm that our models satisfy behavioral calibration for both complete responses and individual claims.

- Adaptive Risk:** In Figure 6, as the risk threshold t increases, the hallucination rate decreases rapidly for models trained with **Verbalized Confidence** and **Critic Value**. Frontier models and Qwen3 trained by standard PPO show convex abstention curves: their boundary between hallucination and abstention areas are convex. In contrast, our models' concave abstention curves indicate a faster adaptation to risk, and consequently, lower hallucination rates.
- Accuracy Preservation:** In Figure 6, at $t = 0$, the policy does not refuse to answer. In Table 1, the accuracy of **Verbalized Confidence** and **Critic Value** is maintained compared to the baseline PPO trained by standard correctness reward.
- Hallucination Reduction:** In Figure 6, the overall hallucination rate is controlled by adaptive abstention. Crucially, at $t = 1$, the hallucination rate drops to 0. Figure 6 also visualizes Signal-to-Noise Ratio (SNR) as the ratio of accuracy (green area) to hallucination (red area). SNR increases drastically for our methods, corresponding to the higher SNR Gain in Table 1 and Table 3.
- Quantitative Calibration:** Analysis of the True Positive (TP) and False Negative (FN) curves in Figure 7 indicates that **Confidence-Brier** and **Critic Value** nearly satisfy behavioral calibration: the TP curve lies above $y = x$, and the FN curve lies below it. In contrast, the curves for frontier models and the base Qwen3 instruct model exhibit more erratic behavior. Their TP rates increase relatively slowly with

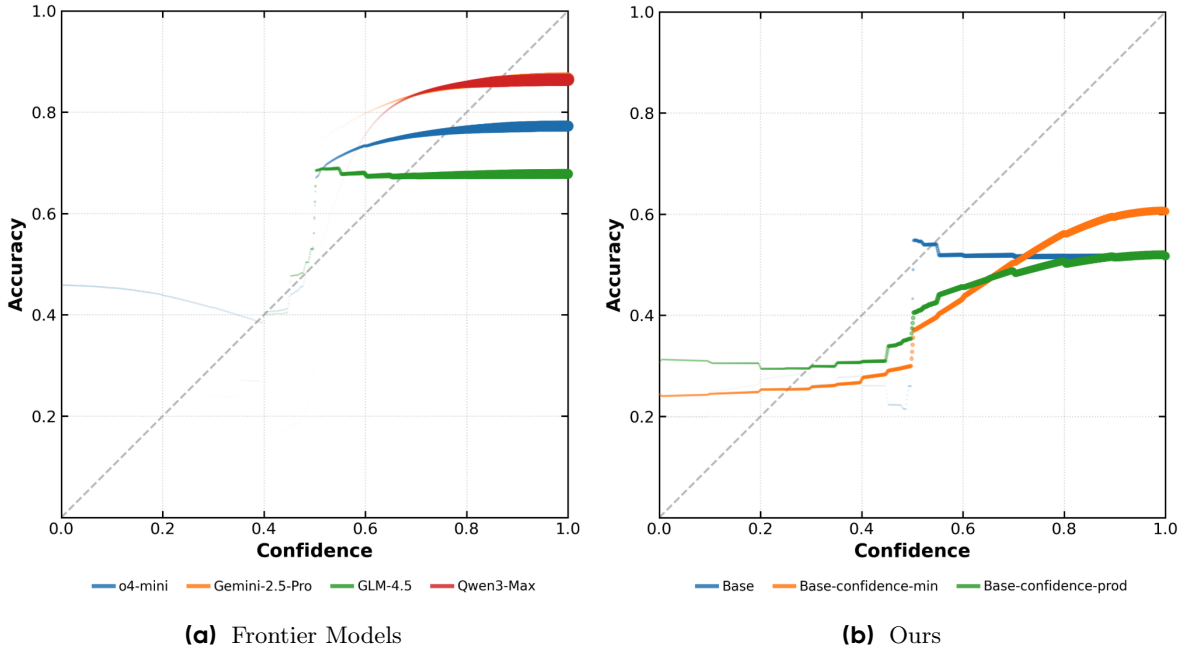


Figure 5 The calibration diagram for claim-level stated confidence on BeyondAIME. The size of curves indicates density. Note that in (a), the curves of Qwen3-Max and Gemini-2.5-Pro are overlapped.

Table 4 Response-level evaluation of confidence calibration on SimpleQA.

Model	SNR Gain \uparrow	Conf AUC \uparrow	Abs Acc \uparrow	smECE \downarrow	Brier \downarrow	NLL \downarrow	Pred Acc \uparrow
Gemini-2.5-pro	0.017	0.556	0.547	0.451	0.436	1.900	0.545
Qwen3-4B-Instruct	0.066	0.561	0.142	0.821	0.762	2.550	0.062
Grok-4	0.147	0.664	0.551	0.307	0.327	0.988	0.492
Qwen3-4B-Instruct-ppo-value	0.211	0.734	0.236	0.665	0.525	1.510	0.031
Claude-sonnet-4.5-nothinking	0.282	0.748	0.544	0.318	0.284	0.786	0.299
GLM-4.6	0.358	0.739	0.518	0.377	0.310	0.878	0.206
Qwen3-4B-Instruct-confidence-Brier	0.411	0.704	0.540	0.459	0.341	1.100	0.058
Claude-sonnet-4.5-thinking	0.456	0.783	0.658	0.200	0.214	0.614	0.308
GPT-5	0.498	0.838	0.729	0.098	0.178	0.530	0.438

the confidence threshold and drop below $y = x$ for highly conservative risk thresholds. These models also over-refuse at relatively low risk thresholds, causing their FN rates to improperly rise above $y = x$.

4.4 Direct Transfer to Factual Question Answering

To test whether the metacognitive ability trained via our method generalizes, we evaluate the model—trained *only* on mathematics—directly on SimpleQA [31], a challenging long-tail factual knowledge benchmark to measure models’ ability to correctly abstain. Results are shown in Table 4.

Despite the model having extremely low prediction accuracy due to model capacity and zero-shot generalization, the confidence calibration of **Confidence-Brier** significantly improves over the base instruct model and rivals frontier models including Gemini-2.5-Pro, Grok-4, and GLM-4.6. **Critic Value** does not generalize as well as **Confidence-Brier** in the cross-domain QA task. It is noteworthy that our methods are more competitive with respect to the SNR Gain and Confidence AUC metric, which is insensitive to the native accuracy of models, making this comparison robust. We successfully trained a transferable “meta-skill” (calibration) that generalizes to new domains even where the model lacks foundational knowledge (accuracy). This proves that calibration is a learnable skill independent of factual knowledge.

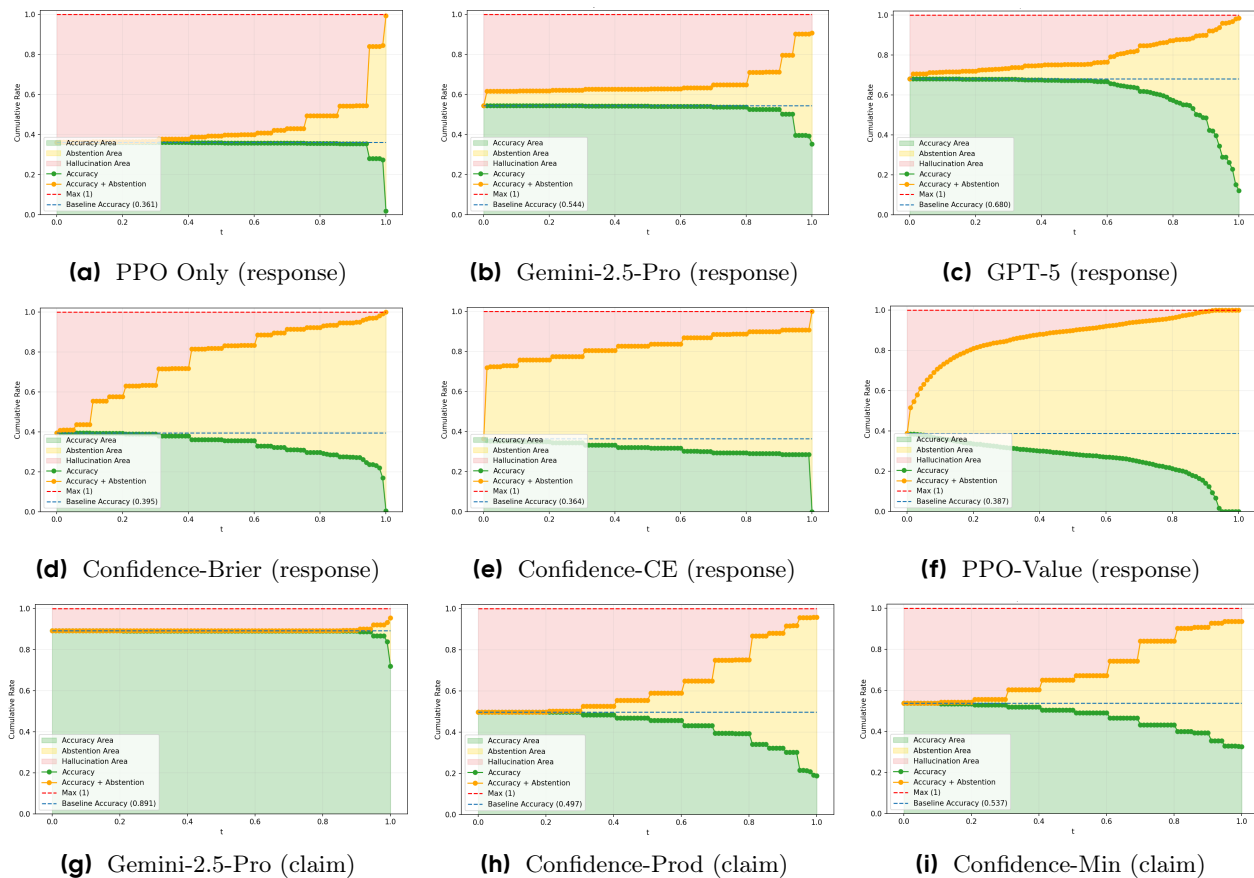


Figure 6 Accuracy, hallucination, and abstention rates obtained by thresholding confidence estimates according to varied risk tolerance t . If the model’s output confidence is less than the risk threshold t , the model refuses to answer. Evaluated on BeyondAIME for both complete responses and individual claims. Baseline accuracy reports the accuracy when always answering.

4.5 Test-Time Scaling

We investigated whether calibrated confidence can be utilized for Test-Time Scaling (TTS), specifically by selecting answers based on *Max Confidence* or *Confidence Weighted Majority*. Our analysis in Figure 8 suggests that the trained confidence acts as a reward proxy better than majority voting, and improves over the verbalized confidence from standard PPO.

However, we discuss a distinction regarding the utility of confidence calibration for TTS. For example, a model generates two guesses for question I—one correct and one incorrect—and assigns a confidence of $\frac{1}{2}$ to both. The model also generates three guesses for question II—one correct and two incorrect—and assigns a confidence of $\frac{1}{3}$ to all of them. The model is perfectly-calibrated, but *Max Confidence* provides no discriminatory power to select the correct answer over the incorrect one. This reveals a fundamental difference in objectives: Behavioral Calibration focuses on inter-prompt discrimination while Test-Time Scaling requires intra-prompt discrimination.

5 Discussion

Our research empirically supports and extends several hypotheses in Kalai et al. [16].

The Inevitability of Hallucination. Language models possess the capacity to selectively refuse generation when uncertainty is high. By implementing dynamic adaptation of rejection rates based on confidence scores,

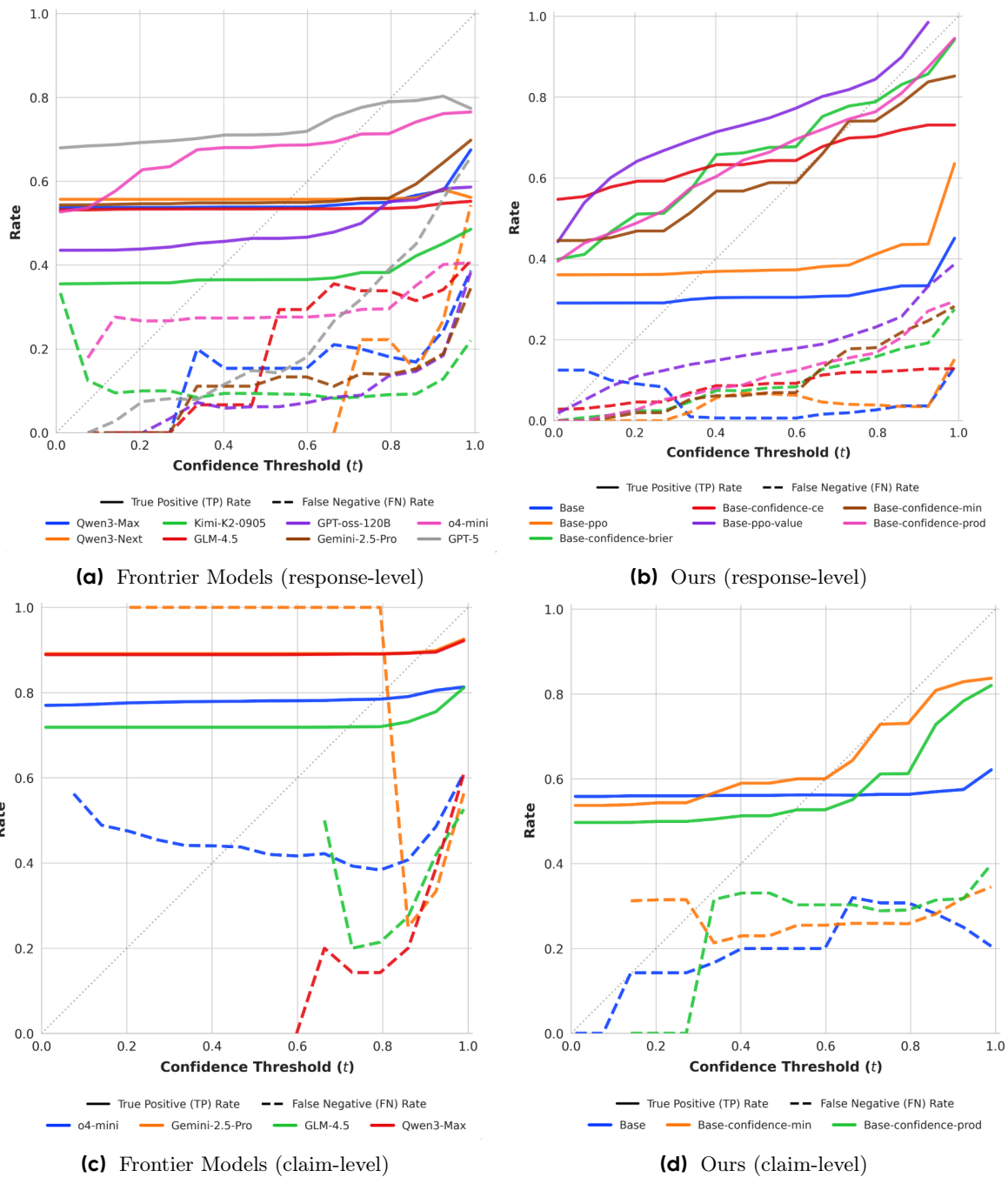


Figure 7 The behavioral calibration diagram for models on BeyondAIME, where we plot the True Positive (bold) and False Negative (dotted) curves. Evaluated for both complete responses and individual claims. Our methods are based on Qwen3-4B-Instruct.

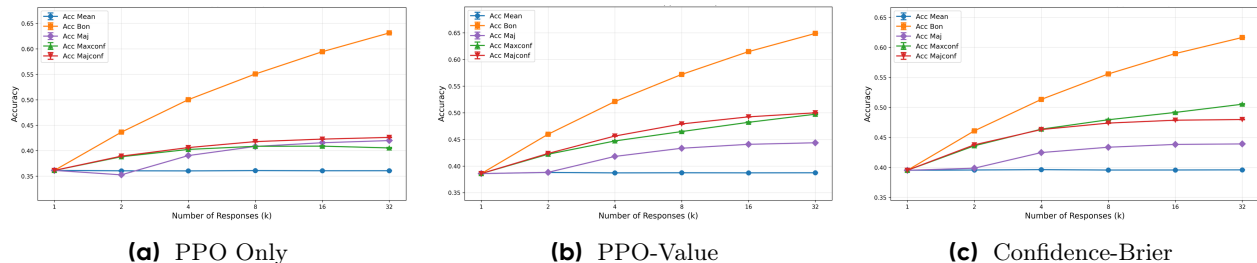


Figure 8 Test-time scaling using confidence as the reward proxy. We select the max-confidence response within k responses (**Maxconf**) or perform weighted majority voting using confidence as weights (**Majconf**). As baselines, accuracy is computed with Mean@ k , Best@ k , and Majority@ k . Evaluated on BeyondAIME [7].

it is possible to maintain maximum performance in “test-taker mode” while ensuring safety in “honest mode”. Crucially, we demonstrate that confidence calibration is a learnable attribute that can be improved through training.

Accuracy versus Hallucination Mitigation. We observe that for several frontier models, accuracy is not positively correlated with hallucination rates or confidence calibration. Notably, the advantage exhibited by GPT series models lies significantly more in their ability to control hallucinations than in their raw accuracy advantage. This indicates that hallucination mitigation is a distinct capability from factual accuracy.

Model Scale versus Hallucination Mitigation. We demonstrate that small models (e.g., 4B parameters) can achieve confidence calibration comparable to frontier models. The computational resources required for effective “calibration” are significantly lower than those needed to pursue absolute accuracy. Conversely, the verbalized confidence of certain large models fail to accurately reflect their actual performance.

We note that small models can assess their limitation more easily (e.g., a small model lacking Maori linguistic data simply refuses, whereas a partially capable model must assess its confidence [16]). Self-verification is most challenging when model accuracy approaches 50% (maximum entropy). Both extremely poor and extremely capable models find self-verification relatively straightforward. To effectively benchmark hallucinations, we evaluate our models where model accuracy (without refusal) is maintained around the 50% threshold. On the BeyondAIME benchmark, Qwen3-4B operates at approximately 40% accuracy, whereas GPT-5 operates at approximately 70%. Consequently, the calibration task is (paradoxically) slightly more difficult for the Qwen3-4B model in this context. The Qwen3-4B model still excels in behavioral calibration.

To facilitate a fair evaluation across models of varying scales and accuracy we employed the AUC metric, demanding that the model’s confidence scores maximally distinguish between positive and negative instances. This metric is robust as it remains insensitive to the average accuracy, providing a pure measure of the model’s introspective capabilities.

References

- [1] Zhipu AI. Glm-4.6: Advanced agentic, reasoning and coding capabilities. Technical report, Zhipu AI, 2025. URL <https://z.ai/blog/glm-4.6>.
- [2] Anthropic. System card: Claude sonnet 4.5. Technical report, Anthropic, 2025. URL <https://www.anthropic.com/claude-sonnet-4-5-system-card>.
- [3] Rahul K Arora, Jason Wei, Rebecca Soskin Hicks, Preston Bowman, Joaquin Quiñonero-Candela, Foivos Tsimpourlas, Michael Sharman, Meghan Shah, Andrea Vallone, Alex Beutel, et al. Healthbench: Evaluating large language models towards improved human health. *arXiv preprint arXiv:2505.08775*, 2025.
- [4] Victor Barres, Honghua Dong, Soham Ray, Xujie Si, and Karthik Narasimhan. τ^2 -bench: Evaluating conversational agents in a dual-control environment. *arXiv preprint arXiv:2506.07982*, 2025.
- [5] Shelly Bensal, Umar Jamil, Christopher Bryant, Melisa Russak, Kiran Kamble, Dmytro Mozolevskyi, Muayad Ali, and Waseem AlShikh. Reflect, retry, reward: Self-improving llms via reinforcement learning. *CoRR*, abs/2505.24726, 2025. doi: 10.48550/ARXIV.2505.24726. URL <https://doi.org/10.48550/arXiv.2505.24726>.
- [6] Jaroslav Blasiok and Preetum Nakkiran. Smooth ECE: principled reliability diagrams via kernel smoothing. In *The Twelfth International Conference on Learning Representations, ICLR 2024, Vienna, Austria, May 7-11, 2024*. OpenReview.net, 2024. URL <https://openreview.net/forum?id=XwiA1nDahv>.
- [7] ByteDance-Seed. Beyondaime: Advancing math reasoning evaluation beyond high school olympiads. <https://huggingface.co/datasets/ByteDance-Seed/BeyondAIME>, 2025.
- [8] Gheorghe Comanici, Eric Bieber, Mike Schaeckermann, Ice Pasupat, Noveen Sachdeva, Inderjit Dhillon, Marcel Blistein, Ori Ram, Dan Zhang, Evan Rosen, et al. Gemini 2.5: Pushing the frontier with advanced reasoning, multimodality, long context, and next generation agentic capabilities. *arXiv preprint arXiv:2507.06261*, 2025.
- [9] Mehul Damani, Isha Puri, Stewart Slocum, Idan Shenfeld, Leshem Choshen, Yoon Kim, and Jacob Andreas. Beyond binary rewards: Training lms to reason about their uncertainty. *CoRR*, abs/2507.16806, 2025. doi: 10.48550/ARXIV.2507.16806. URL <https://doi.org/10.48550/arXiv.2507.16806>.
- [10] Sebastian Farquhar, Jannik Kossen, Lorenz Kuhn, and Yarin Gal. Detecting hallucinations in large language models using semantic entropy. *Nat.*, 630(8017):625–630, 2024. doi: 10.1038/S41586-024-07421-0. URL <https://doi.org/10.1038/s41586-024-07421-0>.
- [11] Yichao Fu, Xuewei Wang, Yuandong Tian, and Jiawei Zhao. Deep think with confidence. *CoRR*, abs/2508.15260, 2025. doi: 10.48550/ARXIV.2508.15260. URL <https://doi.org/10.48550/arXiv.2508.15260>.
- [12] Liang Hu, Jianpeng Jiao, Jiashuo Liu, Yanle Ren, Zhoufutu Wen, Kaiyuan Zhang, Xuanliang Zhang, Xiang Gao, Tianci He, Fei Hu, et al. Finsearchcomp: Towards a realistic, expert-level evaluation of financial search and reasoning. *arXiv preprint arXiv:2509.13160*, 2025.
- [13] Carlos E Jimenez, John Yang, Alexander Wettig, Shunyu Yao, Kexin Pei, Ofir Press, and Karthik Narasimhan. Swe-bench: Can language models resolve real-world github issues? *arXiv preprint arXiv:2310.06770*, 2023.
- [14] Saurav Kadavath, Tom Conerly, Amanda Askell, Tom Henighan, Dawn Drain, Ethan Perez, Nicholas Schiefer, Zac Hatfield-Dodds, Nova DasSarma, Eli Tran-Johnson, Scott Johnston, Sheer El Showk, Andy Jones, Nelson Elhage, Tristan Hume, Anna Chen, Yuntao Bai, Sam Bowman, Stanislav Fort, Deep Ganguli, Danny Hernandez, Josh Jacobson, Jackson Kernion, Shauna Kravec, Liane Lovitt, Kamal Ndousse, Catherine Olsson, Sam Ringer, Dario Amodei, Tom Brown, Jack Clark, Nicholas Joseph, Ben Mann, Sam McCandlish, Chris Olah, and Jared Kaplan. Language models (mostly) know what they know. *CoRR*, abs/2207.05221, 2022. doi: 10.48550/ARXIV.2207.05221. URL <https://doi.org/10.48550/arXiv.2207.05221>.
- [15] Adam Tauman Kalai and Santosh S. Vempala. Calibrated language models must hallucinate. In Bojan Mohar, Igor Shinkar, and Ryan O’Donnell, editors, *Proceedings of the 56th Annual ACM Symposium on Theory of Computing, STOC 2024, Vancouver, BC, Canada, June 24-28, 2024*, pages 160–171. ACM, 2024. doi: 10.1145/3618260.3649777. URL <https://doi.org/10.1145/3618260.3649777>.
- [16] Adam Tauman Kalai, Ofir Nachum, Santosh S. Vempala, and Edwin Zhang. Why language models hallucinate. *CoRR*, abs/2509.04664, 2025. doi: 10.48550/ARXIV.2509.04664. URL <https://doi.org/10.48550/arXiv.2509.04664>.

- [17] Sanyam Kapoor, Nate Gruver, Manley Roberts, Arka Pal, Samuel Dooley, Micah Goldblum, and Andrew Wilson. Calibration-tuning: Teaching large language models to know what they don't know. In *Proceedings of the 1st Workshop on Uncertainty-Aware NLP (UncertainNLP 2024)*, pages 1–14, 2024.
- [18] Stephanie Lin, Jacob Hilton, and Owain Evans. Teaching models to express their uncertainty in words. *Trans. Mach. Learn. Res.*, 2022, 2022. URL <https://openreview.net/forum?id=8s8K2UZGTZ>.
- [19] Xiaoyuan Liu, Tian Liang, Zhiwei He, Jiahao Xu, Wenxuan Wang, Pinjia He, Zhaopeng Tu, Haitao Mi, and Dong Yu. Trust, but verify: A self-verification approach to reinforcement learning with verifiable rewards. *CoRR*, abs/2505.13445, 2025. doi: 10.48550/ARXIV.2505.13445. URL <https://doi.org/10.48550/arXiv.2505.13445>.
- [20] Xin Liu, Muhammad Khalifa, and Lu Wang. Litcab: Lightweight language model calibration over short- and long-form responses. In *The Twelfth International Conference on Learning Representations, ICLR 2024, Vienna, Austria, May 7-11, 2024*. OpenReview.net, 2024. URL <https://openreview.net/forum?id=jH67LHV0IO>.
- [21] Preetum Nakkiran, Arwen Bradley, Adam Golinski, Eugène Ndiaye, Michael Kirchhof, and Sinead Williamson. Trained on tokens, calibrated on concepts: The emergence of semantic calibration in llms. *CoRR*, abs/2511.04869, 2025. doi: 10.48550/ARXIV.2511.04869. URL <https://doi.org/10.48550/arXiv.2511.04869>.
- [22] OpenAI. Gpt-5 system card. Technical report, OpenAI, 2025. URL <https://openai.com/index/gpt-5-system-card/>.
- [23] OpenAI. gpt-oss-120b & gpt-oss-20b model card. *CoRR*, abs/2508.10925, 2025. doi: 10.48550/ARXIV.2508.10925. URL <https://doi.org/10.48550/arXiv.2508.10925>.
- [24] OpenAI. Openai o3 and o4-mini system card. Technical report, OpenAI, 2025. URL <https://openai.com/index/o3-o4-mini-system-card/>.
- [25] Yudi Pawitan and Chris Holmes. Confidence in the reasoning of large language models. *CoRR*, abs/2412.15296, 2024. doi: 10.48550/ARXIV.2412.15296. URL <https://doi.org/10.48550/arXiv.2412.15296>.
- [26] Zhihong Shao, Peiyi Wang, Qihao Zhu, Runxin Xu, Junxiao Song, Mingchuan Zhang, Y. K. Li, Y. Wu, and Daya Guo. Deepseekmath: Pushing the limits of mathematical reasoning in open language models. *CoRR*, abs/2402.03300, 2024. doi: 10.48550/ARXIV.2402.03300. URL <https://doi.org/10.48550/arXiv.2402.03300>.
- [27] Paul Stangel, David Bani-Harouni, Chantal Pellegrini, Ege Özsoy, Kamilia Zaripova, Matthias Keicher, and Nassir Navab. Rewarding doubt: A reinforcement learning approach to calibrated confidence expression of large language models. *arXiv preprint arXiv:2503.02623*, 2025.
- [28] Amir Taubenfeld, Tom Sheffer, Eran Ofek, Amir Feder, Ariel Goldstein, Zorik Gekhman, and Gal Yona. Confidence improves self-consistency in llms. In Wanxiang Che, Joyce Nabende, Ekaterina Shutova, and Mohammad Taher Pilehvar, editors, *Findings of the Association for Computational Linguistics, ACL 2025, Vienna, Austria, July 27 - August 1, 2025*, pages 20090–20111. Association for Computational Linguistics, 2025. URL <https://aclanthology.org/2025.findings-acl.1030/>.
- [29] Kimi Team, Yifan Bai, Yiping Bao, Guanduo Chen, Jiahao Chen, Ningxin Chen, Ruijue Chen, Yanru Chen, Yuankun Chen, Yutian Chen, et al. Kimi k2: Open agentic intelligence. *arXiv preprint arXiv:2507.20534*, 2025.
- [30] Qwen Team. Qwen3 technical report, 2025. URL <https://arxiv.org/abs/2505.09388>.
- [31] Jason Wei, Nguyen Karina, Hyung Won Chung, Yunxin Joy Jiao, Spencer Papay, Amelia Glaese, John Schulman, and William Fedus. Measuring short-form factuality in large language models. *CoRR*, abs/2411.04368, 2024. doi: 10.48550/ARXIV.2411.04368. URL <https://doi.org/10.48550/arXiv.2411.04368>.
- [32] xAI. Grok 4 model card. Technical report, xAI, 2025. URL <https://data.x.ai/2025-08-20-grok-4-model-card.pdf>.
- [33] Qiyang Yu, Zheng Zhang, Ruofei Zhu, Yufeng Yuan, Xiaochen Zuo, Yu Yue, Tiantian Fan, Gaohong Liu, Lingjun Liu, Xin Liu, Haibin Lin, Zhiqi Lin, Bole Ma, Guangming Sheng, Yuxuan Tong, Chi Zhang, Mofan Zhang, Wang Zhang, Hang Zhu, Jinhua Zhu, Jiase Chen, Jiangjie Chen, Chengyi Wang, Hongli Yu, Weinan Dai, Yuxuan Song, Xiangpeng Wei, Hao Zhou, Jingjing Liu, Wei-Ying Ma, Ya-Qin Zhang, Lin Yan, Mu Qiao, Yonghui Wu, and Mingxuan Wang. DAPO: an open-source LLM reinforcement learning system at scale. *CoRR*, abs/2503.14476, 2025. doi: 10.48550/ARXIV.2503.14476. URL <https://doi.org/10.48550/arXiv.2503.14476>.
- [34] Aohan Zeng, Xin Lv, Qinkai Zheng, Zhenyu Hou, Bin Chen, Chengxing Xie, Cunxiang Wang, Da Yin, Hao Zeng, Jijie Zhang, Kedong Wang, Lucen Zhong, Mingdao Liu, Rui Lu, Shulin Cao, Xiaohan Zhang, Xuancheng Huang,

- Yao Wei, Yean Cheng, Yifan An, Yilin Niu, Yuanhao Wen, Yushi Bai, Zhengxiao Du, Zihan Wang, Zilin Zhu, Bohan Zhang, Bosi Wen, Bowen Wu, Bowen Xu, Can Huang, Casey Zhao, Changpeng Cai, Chao Yu, Chen Li, Chendi Ge, Chenghua Huang, Chenhui Zhang, Chenxi Xu, Chenzheng Zhu, Chuang Li, Congfeng Yin, Daoyan Lin, Dayong Yang, Dazhi Jiang, Ding Ai, Erle Zhu, Fei Wang, Gengzheng Pan, Guo Wang, Hailong Sun, Haitao Li, Haiyang Li, Haiyi Hu, Hanyu Zhang, Hao Peng, Hao Tai, Haoke Zhang, Haoran Wang, Haoyu Yang, He Liu, He Zhao, Hongwei Liu, Hongxi Yan, Huan Liu, Huilong Chen, Ji Li, Jiajing Zhao, Jiamin Ren, Jian Jiao, Jiani Zhao, Jianyang Yan, Jiaqi Wang, Jiayi Gui, Jiayue Zhao, Jie Liu, Jijie Li, Jing Li, Jing Lu, Jingsen Wang, Jingwei Yuan, Jingxuan Li, Jingzhao Du, Jinhua Du, Jinxin Liu, Junkai Zhi, Junli Gao, Ke Wang, Lekang Yang, Liang Xu, Lin Fan, Lindong Wu, Lintao Ding, Lu Wang, Man Zhang, Minghao Li, Minghuan Xu, Mingming Zhao, and Mingshu Zhai. GLM-4.5: agentic, reasoning, and coding (ARC) foundation models. *CoRR*, abs/2508.06471, 2025. doi: 10.48550/ARXIV.2508.06471. URL <https://doi.org/10.48550/arXiv.2508.06471>.
- [35] Zhiyuan Zeng, Jiashuo Liu, Siyuan Chen, Tianci He, Yali Liao, Yixiao Tian, Jinpeng Wang, Zaiyuan Wang, Yang Yang, Lingyue Yin, et al. Futurex: An advanced live benchmark for llm agents in future prediction. *arXiv preprint arXiv:2508.11987*, 2025.
- [36] Kaiwen Zha, Zhengqi Gao, Maohao Shen, Zhang-Wei Hong, Duane S. Boning, and Dina Katabi. RL tango: Reinforcing generator and verifier together for language reasoning. *CoRR*, abs/2505.15034, 2025. doi: 10.48550/ARXIV.2505.15034. URL <https://doi.org/10.48550/arXiv.2505.15034>.
- [37] Xiaoling Zhou, Mingjie Zhang, Zhemg Lee, Wei Ye, and Shikun Zhang. Hademif: Hallucination detection and mitigation in large language models. In *The Thirteenth International Conference on Learning Representations, ICLR 2025, Singapore, April 24-28, 2025*. OpenReview.net, 2025. URL <https://openreview.net/forum?id=VwOYxPScxB>.